DOE/ET/20279-207

ELECTRICAL ASPECTS OF PHOTOVOLTAIC-SYSTEM SIMULATION

G.W. Hart
P. Raghuraman

June 1982

Massachusetts Institute of Technology
Lincoln Laboratory
Lexington, Massachusetts 02173-0073

Prepared for
THE U.S. DEPARTMENT OF ENERGY
UNDER CONTRACT NO. DE-AC02-76ET20279

DOE/ET/20279--207

DE82 021956

DOE/ET/20279-207

Distribution Category UC 63a-e

ELECTRICAL ASPECTS OF PHOTOVOLTAIC-SYSTEM SIMULATION

G.W. Hart

P. Raghuraman

June 1982

Massachusetts Institute of Technology

Lincoln Laboratory

Lexington, Massachusetts 02173-0073

Prepared for

THE U.S. DEPARTMENT OF ENERGY

UNDER CONTRACT NO. DE-AC02-76ET20279

ABSTRACT

A TRNSYS simulation has been developed to simulate the performance of utility-interactive residential photovoltaic energy systems. The PV system is divided into its major functional components, which are individually described with computer models. These models are described in detail. The results of simulation and actual measured data obtained at MIT Lincoln Laboratory's Northeast Residential Experiment Station are compared. The electrical influences on the design of such photovoltaic energy systems are given particular attention.

Blank Page

TABLE OF CONTENTS

LIST OF FIGURES

1.0 INTRODUCTION

MIT Lincoln Laboratory, under the aegis of the U.S. Department of Energy (DOE), has established the Northeast Residential Experiment Station (NE RES) in Concord, Massachusetts, to develop and then monitor the performance of state-of-the-art residential solar photovoltaic (PV) energy systems. Five prototype residential PV systems at the NE RES are presently under test. Each of these Prototype Systems consists of a roof-mounted PV array, sized to meet at least 50% of the annual electrical demand of an energy-conserving house, and an enclosed structure to house the remainder of the PV system equipment and test instrumentation. Four of these PV systems were designed and built by industry participants in the Lincoln Laboratory project; the fifth prototype was designed in-house. Table I describes the features of the PV energy systems at the NE RES. Note that these parameters are applicable only up until December 1981. Starting at that time, a number of the prototypes were electrically reconfigured.

TABLE I

NORTHEAST RESIDENTIAL EXPERIMENT STATION PV SYSTEMS CHARACTERISTICS

Prototype System	Lincoln Lab	Westinghouse	General Electric	TriSolarCorp	Solarex
Module Supplier:	Solarex	ARCO Solar	GE	Applied Solar	Solarex
Array Area (m^2)	85.0	69.2	76.8	47.2	68.3
Array Peak Power (kW)	6.8	5.1	6.7	4.8	5.0
Open-Circuit Voltage (V)	253	250	257	234	240
Short-Circuit Current (A)	37.4	25.1	26.9	21.7	23.7
Maximum Power Voltage (V)	190	185	197	190	182
Maximum Power Current (A)	33.3	22.2	23.3	19.9	20.3
α (A/Deg C)	.063	.0154	.0105	.0128	.027
β (V/Deg C)	1.198	1.02	1.24	1.08	1.11
Series Resistance (Ohms)	1.34	1.93	1.44	1.28	1.6
Reference Insolation (kW/m^2)	1.	.83	.78	.82	.80
Reference Temperature (°C)	56	44	47	38	34
Inverter Manufacturer	Gemini	Abacus	Abacus	Gemini	Abacus
Inverter Size (kVA)	8	6	6	8	6

The arrays provide dc energy which is converted to ac energy by power-conditioning equipment in order to service all the usual loads of a residence. All the Prototype Systems are utility interactive; excess solar-generated electric energy is fed back to the local utility grid, thereby eliminating the need for on-site storage.

Packaged programs capable of modelling PV systems include TRNSYS[1] and Solcel-II[2]. The present work was undertaken in order to provide a more versatile program, which can model each of the electrical components of the system. The models are detailed enough to allow one to assess quantitatively the effect of varying the electrical operation of each of the components. This is part of an ongoing DOE project to simulate and assess the performance of residential PV energy systems of different designs when placed at different locations across the United States.

The present work describes a TRNSYS simulation that has been developed to simulate the performance of such PV energy systems. TRNSYS (standing for Transient Simulation) is a computer simulation program package developed at the Solar Energy Laboratory of the University of Wisconsin at Madison.

Figure 1 shows the basic elements of a utility-interactive residential PV energy system. For simulation purposes, each system is divided into its major functional components, which are individually described with computer models:

(1) A detailed thermal model of an array. This computes cell temperature, given insolation, ambient temperature and wind speed.

(2) A model of an array's dc current-voltage characteristics as a function of insolation and cell temperature;

(3) Models of the electrical characteristics of the dc side of power conditioners (devices which convert dc to ac); and

(4) Models of power conditioner ac output, given the dc input.

A TRNSYS compatible subroutine has been written for each of these components.

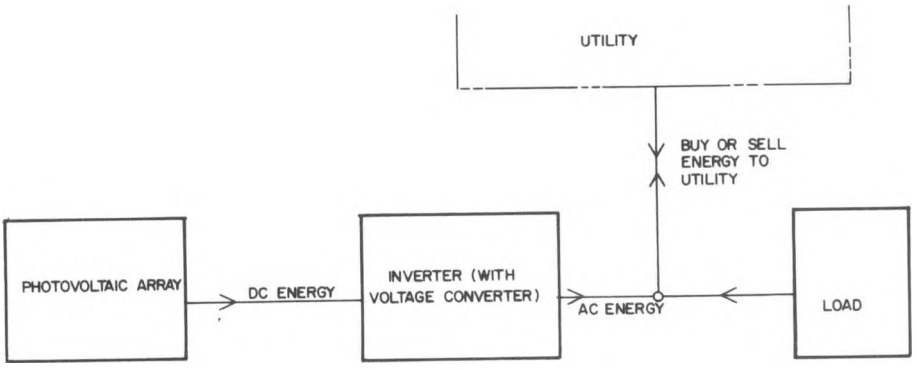

Figure 1. Utility-interactive photovoltaic energy system.

The overall organization of the program and the details of the three electrical components are presented below. A companion report (Reference 3), describes several models that can be used for the thermal portion (1) of the simulation. The entire simulation has been well calibrated and verified against measured thermal and electrical performance of prototypes at the NE RES.

The following sections describe the organization of the simulation and the three electrical components. Each part is compared in detail to actual data measured at NE RES prototypes. The components are described in the order listed above (2,3,4). The general framework provided by TRNSYS is described first.

2.0 SIMULATION AND MODELLING OF COMPONENTS

The simulation is organized within the framework of TRNSYS. Figure 2 shows the organization of the simulation. The independent variables are the physical quantities needed to run the simulation which can be classified into weather and load data. The weather data determine the performance of the PV energy system (inverter ac output), while the load data determine whether energy has to be bought or sold to the utility.

C74-1651

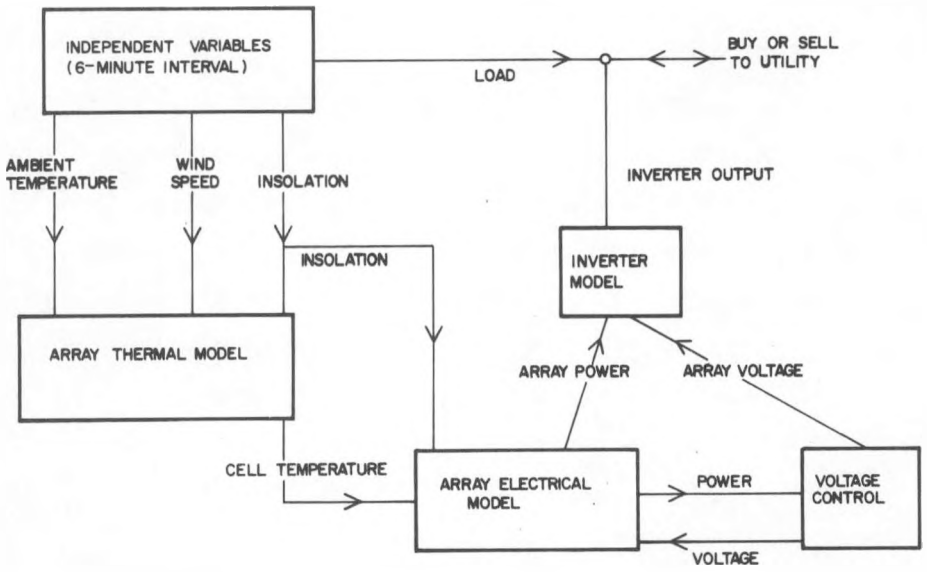

Figure 2. Organization of simulation.

TRNSYS provides a convenient computational framework for a number of reasons. It provides for convergence control over the different subroutines. The functional components of the system are each represented by a subroutine which models its input-output characteristics. TRNSYS allows these inputs and outputs to be flexibly interconnected, and sees to it that the different subroutines are called as often as necessary until all variables converge to stable values. TRNSYS also provides simple mechanisms for converting units allowing, for example, a subroutine written with inputs and outputs in SI units to be connected with a subroutine using English units, with no internal changes to either subroutine. In addition, TRNSYS provides standard subroutines that perform standard calculations; e.g., a radiation subroutine which computes the insolation on a tilted surface given the insolation on a horizontal surface.

TRNSYS also provides for a time frame for the simulation. The results described are obtained with 24-hour simulations at six-minute intervals based on weather and residential load data measured at the NE RES. These simulations are used for calibrating and checking the validity of the analysis. Other runs are made over a year-long period at hourly intervals using Typical Meteorological Year (TMY) and SOLMET data. These are used for projecting typical annual performance.

3.0 NOMENCLATURE FOR I-V CURVE DESCRIPTION

α	Current change temperature coefficient at reference insolation (Amps/°C)	
β	Voltage change temperature coefficient (Volts/°C)	
C_1, C_2	Constants used by the TRW model, defined in equation (2)	
I	Array Current	(Amps)
I_{mp}	Array Maximum Power Current	(Amps)
I_{sc}	Array Short Circuit Current	(Amps)
L	Total Tilt Insolation	(kW/m^2)
L_{ref}	Reference Insolation	(kW/m^2)
R_s	Array Series Resistance	(Ohms)
T	Cell temperature	(°C)
T_{ref}	Reference cell temperature	(°C)
ΔT	Change in cell temperature	(°C)
V	Array Voltage (Volts)	
V_{mp}	Array Maximum Power Voltage	(Volts)
V_{oc}	Array Open-Circuit Voltage	(Volts)

4.0 ARRAY CURRENT-VOLTAGE CHARACTERISTICS

The I-V characteristics of a PV array are modeled with the "TRW" model[4]. This model requires data defining three points from a measured I-V curve of the array to be modeled: the open-circuit voltage, the short-circuit current, and the maximum power point. The model fits an exponential curve to these points and interpolates between them to provide a complete I-V curve in analytical form. Analytically, the array current, I, is given as a function of the array voltage, V, by

$$I = I_{sc}\left[1 - C_1\left(e^{\left\{\frac{V}{C_2 V_{oc}}\right\}} - 1\right)\right] \qquad (1)$$

where

$$C_1 = \left(1 - \frac{I_{mp}}{I_{sc}}\right) e^{\frac{-V_{mp}}{C_2 V_{oc}}}$$

$$C_2 = \frac{\frac{V_{mp}}{V_{oc}} - 1}{\ell n\left(1 - \frac{I_{mp}}{I_{sc}}\right)}. \qquad (2)$$

Where I_{sc} is the short-circuit current, V_{oc} is the open-circuit voltage and I_{mp}, V_{mp} are the maximum-power-point current and voltage. The constants C_1 and C_2 can be evaluated once at the beginning of the simulation; then only Equation 1 need be computed at each time step. Particular values of these parameters for each of the five NE RES prototypes are given in Table I.

Figure 3 compares an I-V curve measured on one string of the Lincoln array with the I-V curve generated by the TRW model based on three points. Although the simulated curve can be seen to pass through the three given points, the curve is not of the exact shape required. This error remains uncorrected in the simulation.

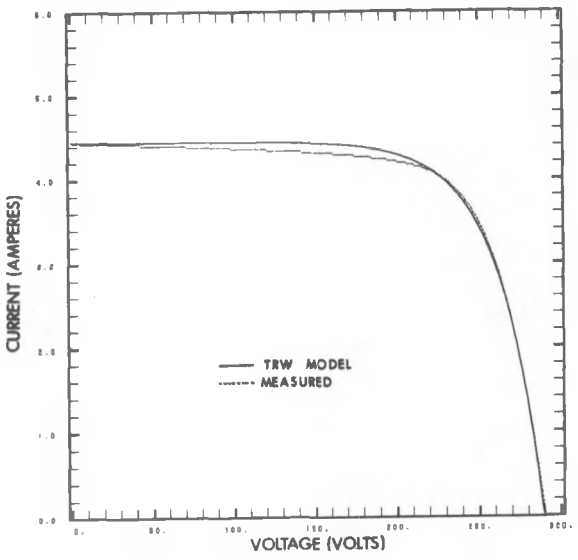

Figure 3. Simulated and measured reference I-V curve.

The curve of Fig. 3 is an arbitrary reference I-V curve. It is only applicable at one particular insolation level and cell temperature. The simulation uses the "Sandstrom" model[5] to translate this curve to other insolations and temperatures. This model shifts the given curve left or right, and up or down as a function of these two variables, but does not alter its shape. Figure 4 shows how this model translates I-V curves. The top two curves of the figure are for an insolation of 1 kW/m^2. The lower two are for half that insolation value. In each of these pairs the curve to the right is for a cell temperature of 30°C. The curves to the left are for a cell temperature of 60°C. The model shifts any point (V_{ref}, I_{ref}) of the reference IV curve to a new point, (V,I). The curve is translated as a template, without distorting its shape, according to Equation 3:

$$\Delta T = T - T_{ref}$$

$$\Delta I = \alpha \left(\frac{L}{L_{ref}}\right) \Delta T + \left(\frac{L}{L_{ref}} - 1\right) I_{sc}$$

$$\Delta V = -\beta \Delta T - R_s \Delta I \qquad (3)$$

$$V_{new} = V_{ref} + \Delta V$$

$$I_{new} = I_{ref} + \Delta I$$

The variables are defined above in the nomenclature section. The exact values of these parameters needed to evaluate Equations 3 are given in Table I.

C74-1903

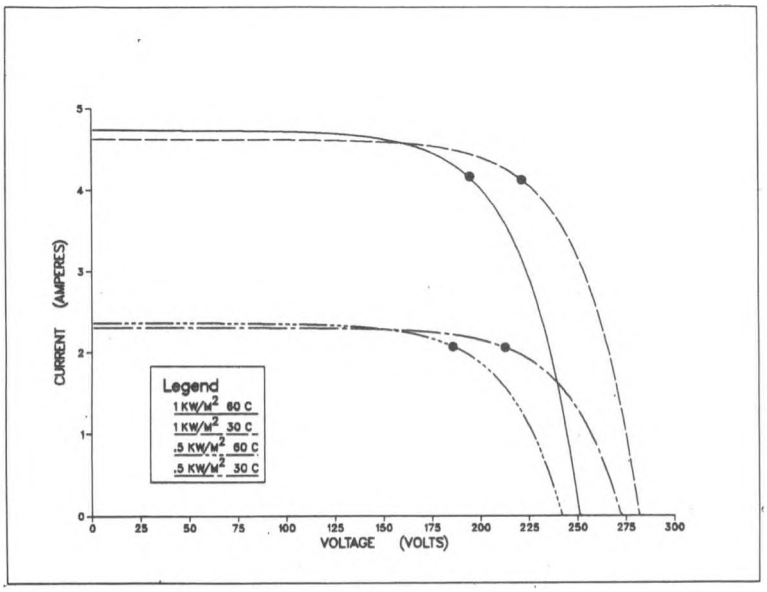

Figure 4. Simulation of translation of I-V curves.

When computing the current output on a translated I-V curve for some specific operating voltage, V, it is not necessary to translate the entire curve to the insolation and cell temperature conditions. Given the reference current vs voltage function, I(V), defined by Equation 1, the translated function, $I'(V_{new})$, is evaluated as $I\ (V_{new} - \Delta V) + \Delta I$.

To evaluate this model, we compare measured I-V curves at a variety of ambient conditions, with the curves defined by Equations 1 through 3. Figure 5 shows a sampling of measured I-V curves paired with the translations of Fig. 3 that the model predicts for the appropriate insolation and cell temperatures. The error in the shape of Fig. 3 remains visible in some of these curves, but the curves translate appropriately.

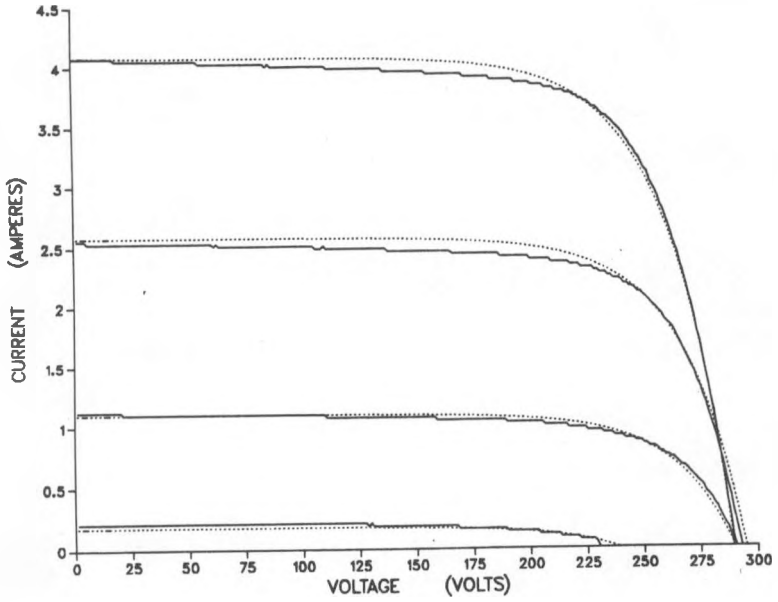

Figure 5. Simulated and measured I-V curves.

5.0 ARRAY VOLTAGE CONTROL

The simulation is capable of operating with three distinct array voltage control strategies: fixed voltage, maximum-power-point tracking, and a hybrid method used by the Windworks Gemini inverter. None of the prototypes at the NE RES has an inverter which is operated in a fixed voltage mode. There are three Abacus inverters, which are designed to maximum-power-point track, and two Geminis as of this writing. The curve of Fig. 6 shows the basic shape of the DC current-voltage characteristics which the Gemini inverter imposes on the array. The point at which the curve begins to rise, and the point where it levels off are manually set on the inverter, and are parameters to the modeling subroutine. The scattered points of Fig. 6 are measured values of current versus voltage which were used to calibrate the model.

C74-2039

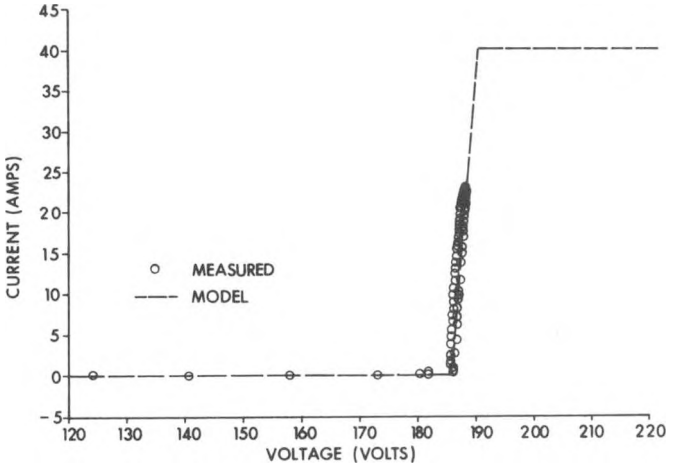

Figure 6. Gemini inverter dc I-V characteristics.

Voltage is determined by a voltage control subroutine which is indicated on the lower right of Fig. 2. The subroutine uses an analytical expression of power versus voltage that is implied by the current versus voltage plot (Fig. 6). The subroutine outputs the voltage level appropriate for any input power level. The TRNSYS controller algorithm iteratively calls the voltage control subroutine and the array current-voltage subroutine until a power and voltage is determined which is consistent with both subroutines.

Figure 7 shows how the Gemini varies the array voltage across time, and the corresponding voltage that is predicted by the simulation. The discrepancies that occur at times of low insolation arise from slight calibration error or instability in the hardware which measures the tilt insolation. The simulated inverter is very sensitive to insolation, and "wakes up" before there is sufficient light to affect the actual inverter. Although the discrepancy appears to be significant, it actually results in a negligible power difference because the insolation is so low at these times.

The Abacus inverters attempt to find the maximum-power-point voltage for the array. Prior to December 1981, they used a searching method which resulted in oscillations around the true maximum power voltage. Figure 8 compares the array voltage selected by the inverter with the calculated maximum power voltage. The significant difference between the model and the measured voltage is attributed to the fact that the inverter was not truly maximum-power-point tracking.

C74-2047

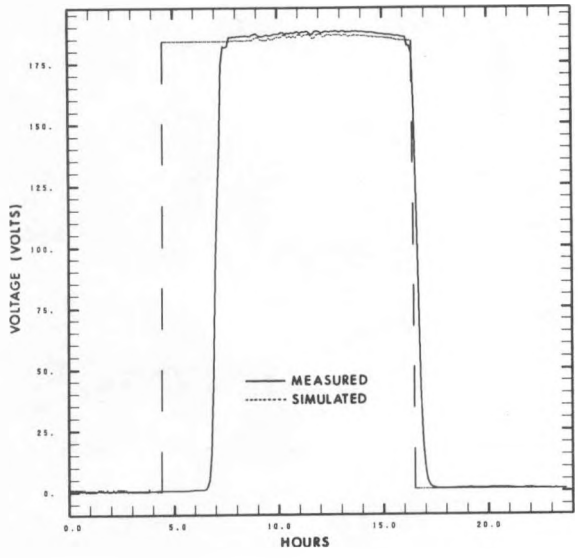

Figure 7. Measured and simulated array voltage for Gemini inverter.

C74-1920A

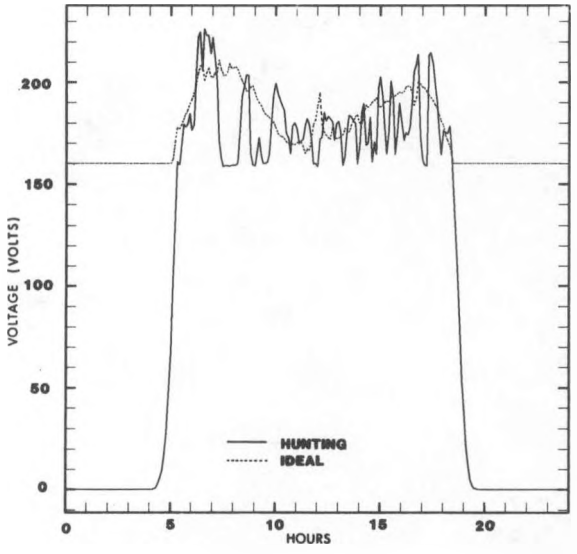

Figure 8. Measured and simulated array voltage for Abacus inverter with "searching" maximum-power-point tracker.

During December 1981, the Abacus inverters were modified to use a "pilot cell" approach. The array voltage was set to a fixed multiple of the open circuit voltage of one cell (or module). For this to work, the multiple must be properly set. Figure 9 shows the array voltage calculated in this manner with the predicted maximum-power voltage of the Westinghouse array. They differ at sunrise for a short period before the inverter "wakes up."

C74-2046

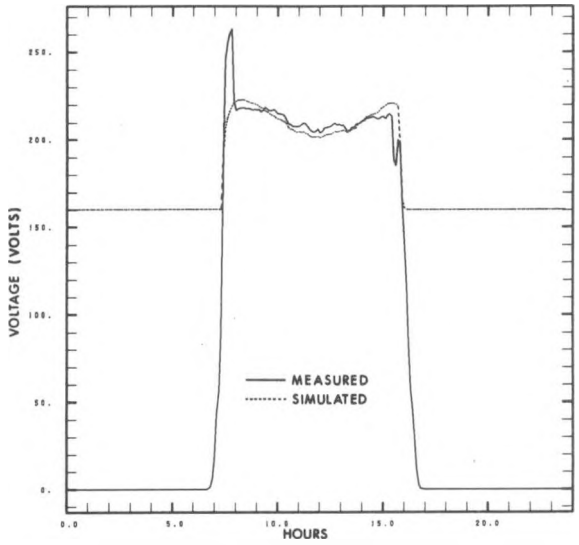

Figure 9. Measured and simulated array voltage for Abacus inverter with "pilot cell" maximum-power-point tracker.

For both of the above methods, the searching algorithm and the pilot cell method, the simulation simply searches through the I-V curve for the maximum power. No attempt has been made to simulate these systems when they do not behave optimally.

The various aspects of the array modeling discussed above can be checked together by comparing the array dc power with the predicted array power across time. Figure 10 makes the comparison for the TriSolar prototype for the same day as Fig. 7. A total electrical output of 18.6 kWh was predicted, compared to a measured output of 18.2 kWh. The exact value varies from day to day; the worst-case difference between measured and predicted values is less than 5%.

C74-2045

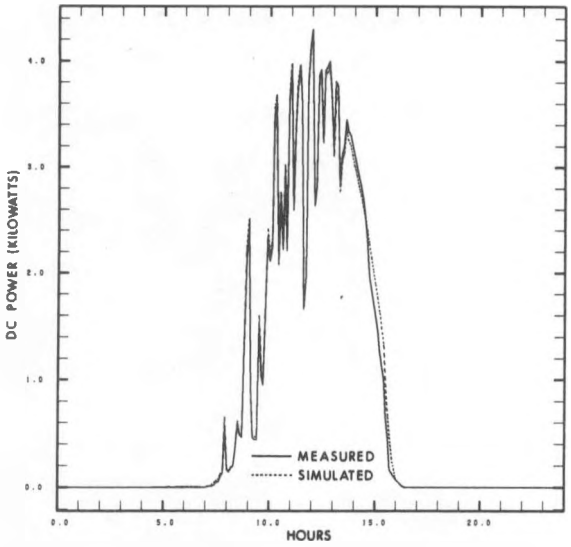

Figure 10. Measured and simulated dc power output from the TriSolar array.

C74-2044

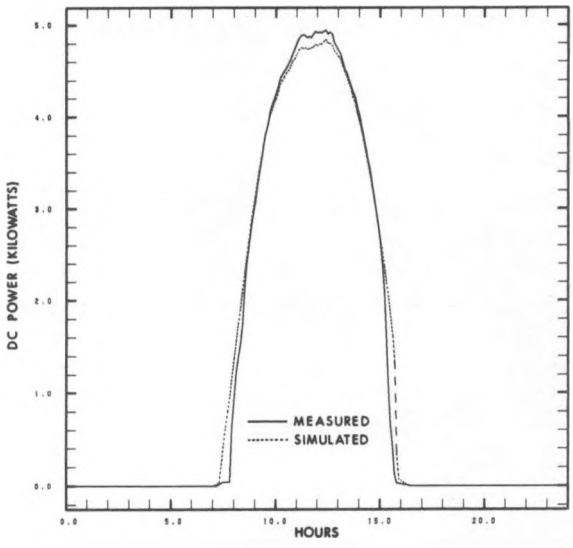

Figure 11. Measured and simulated dc power output from the Westinghouse array.

Figure 11 shows the measured and predicted dc power for the Westinghouse array on the same day that is shown in Fig. 9. The measured and predicted energy outputs are 29.8 and 29.0 kWh, respectively. This is a 2.8% error.

6.0 INVERTER EFFICIENCY

The efficiency of the two inverters modeled is calculated as a function of dc power and dc voltage. A set of measurements was taken over the operating range of powers and voltages that can be expected. These values are shown in Fig. 12 for the Gemini inverter, and in Fig. 13 for the Abacus. The inverter model is given a voltage and power level and interpolates within the given efficiency data.

C74-2040

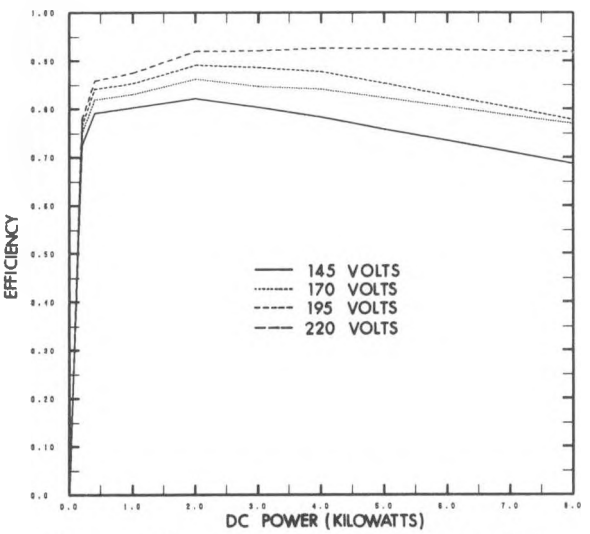

Figure 12. Efficiency of Gemini inverter (with isolation transformer).

C74-2041

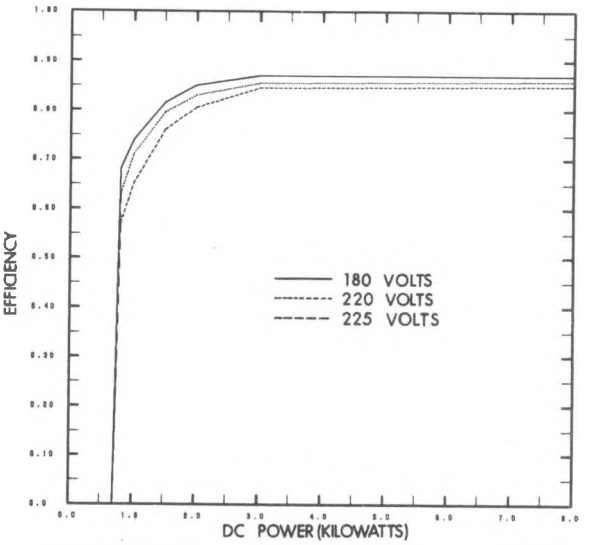

Figure 13. Efficiency of Abacus inverter.

A standard two-dimensional linear interpolation formula is used. The data of Fig. 12 and 13 are provided for a set of voltages, V_i, and a set of input powers, P_j. For each pair V_i, P_j, the efficiency, $\eta(i,j)$ is specified. The algorithm calculates an appropriate η for any arbitrary voltage, V, and power, P, by first locating i and j such that

$$V_i \leq V \leq V_{i+1}$$

and

$$P_j \leq P \leq P_{j+1}$$

and then evaluating Equations 4:

$$f_v = \frac{V - V_i}{V_{i+1} - V_i} \qquad f_p = \frac{P - P_i}{P_{i+1} - P_i}$$

$$\eta = f_v f_p \eta(i+1, j+1) + f_v(1-f_p)\eta(i+1,j) + (1-f_v) f_p \eta(i,j+1) + (1-f_v)(1-f_p)\eta(i,j). \quad (4)$$

The output power is then calculated as η times the input power.

There is also a tare loss, P_{tare}, associated with each inverter. If the output as calculated above, ηP, is zero, then the tare loss is used as the output. Thus the output power, P_{out}, is given by:

$$P_{out} = \begin{cases} \eta P & \text{if } \eta P > 0 \\ P_{tare} & \text{if } \eta P = 0. \end{cases}$$

Note that P_{tare} is less than zero.

The measured ac output of an inverter can be compared with the predicted power as they vary in time. Figure 14 compares the measured and predicted inverter output of the TriSolar array for one day. Figure 15 does the same for the Westinghouse array. There is a 3.3% error in the TriSolar case and a 4.7% error in the Westinghouse case.

C74-2043

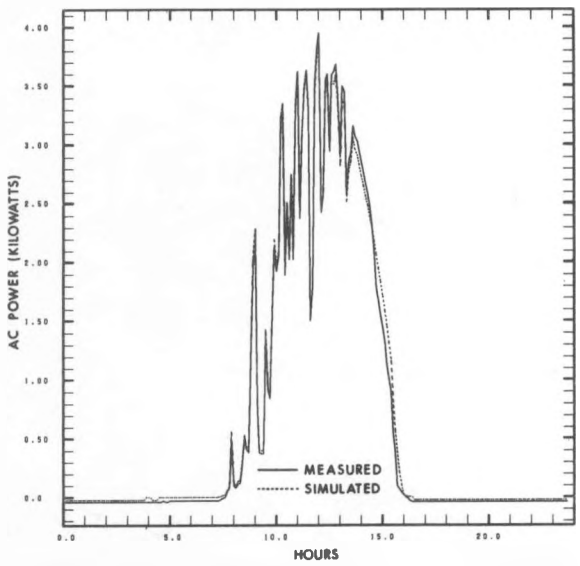

Figure 14. Measured and simulated ac power output of Gemini inverter.

C74-2042

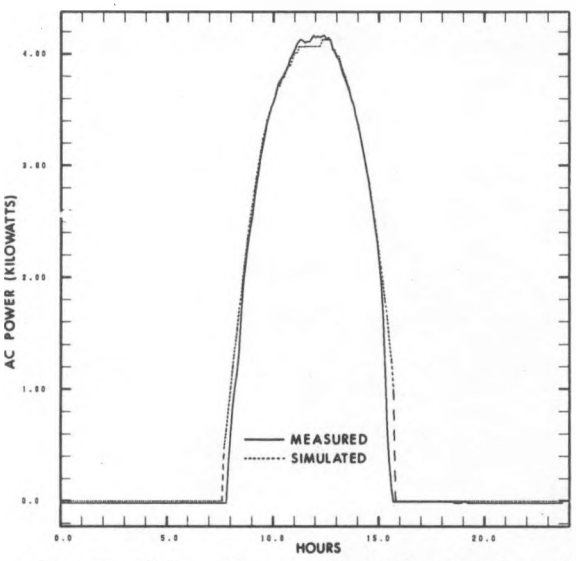

Figure 15. Measured and simulated ac power output of Abacus inverter.

These accuracies are typical for the simulation. It is possible to predict system output consistently within a 5% error. This is the highest accuracy that we can hope to attain and verify because the data-gathering system which provides measured data against which to compare the simulation cannot be guaranteed to have an error of less than 5%. The error in the data system is due to drift in the calibration of the sensors.

The error in the simulation is attributed to approximating assumptions in some of the models (especially the I-V reference curve problem shown in Fig. 3) and inaccuracies in the measurement of system parameters (such as those given in Table I). A further problem comes about from the fact that pyranometer readings represent a wider spectral band than that to which solar cells are sensitive so that the effective insolation "seen" by the PV array is not directly proportional to the pyranometer reading. Although the simulation is occasionally in error by up to 5%, it is as accurate as our measurements can verify. The remaining discrepancy between the simulation and the measured data is not worth pursuing further because the second-order effects listed above limit the resulting accuracy to 5%.

REFERENCES

1. Klein, S. A., et al., "TRNSYS--A Transient System Simulation User's Manual," University of Wisconsin-Madison, Engineering Experiment Station Report 38-10 (1979).

2. Hoover, E. R., "SOLCEL-II: An Improved Photovoltaic System Analysis Program," SAND79-1785, Sandia Laboratories, February 1980.

3. Hart, G. W. and Raghuraman, P., "Residential Photovoltaic System Simulation: Thermal Aspects," proceedings of the ASME Solar Energy Division Fourth Annual Technical Conference, Albuquerque, NM, 26-30 April 1982.

4. Luft, W., Barton, J. R. and Conn, A.A., "Multifaceted Solar Array Performance Determination," TRW Systems Group, Redondo Beach, CA, February 1967.

5. Solar Cell Array Design Handbook, Volume 1, 9.2, (Jet Propulsion Laboratory), reproduced by National Technical Information Service, U.S. Dept. of Commerce, Springfield, Virginia, #N77-14193.